Pergamon

Int. J. Solids Structures Vol. 33, No. 10, pp. 1375–1386, 1996

0020-7683/96 $15.00 + .00

0020-7683(95)00102-6

CYLINDRICAL SHELL SUBJECT TO LOCAL LOADS APPLIED ON AN ARBITRARILY SHAPED AREA

L. S. ONG† and S. T. JOHN CHEUNG
School of Mechanical and Production Engineering Nanyang Technological University, Nanyang Avenue, Singapore 2263

and

A. S. TOOTH
Department of Mechanical Engineering, University of Strathclyde, U.K.

(*Received* 15 *November* 1994; *in revised form* 17 *April* 1995)

Abstract—The problem of a cylindrical shell subject to local loads over an arbitrary shaped base is being analysed. Governing equations for the cylindrical shell are solved by the double Fourier series expansion technique, yielding solutions for stresses and displacements in terms of Fourier load coefficients. The load coefficients are double integral functions, which have variable integral limits when the load has a non-rectangular base profile. To evaluate the load coefficients, two methods are studied. In the first method, the discrete Fourier approximation technique is employed. In the second method, the double integral expression is converted into a boundary line integral by means of Green's Theorem. For a boundary with no analytical expression, it can be approximated by a series of line segments and integration is carried out along each line segment. The numerical integration is accomplished by the Clenshaw-Curtis quadrature rule. The boundary integral method is simpler and easier to implement in the computer than the discrete Fourier approximation method.

NOTATION

A	$Et/(1-\nu^2)$
$2a$	axial length of rectangular patch load
$2c$	circumferential width of patch load
E	Young's modulus of elasticity
k	$t^2/12r^2$
L	length of cylinder
M_x, M_ϕ	moment stress resultants
N_x, N_ϕ	direct stress resultants
NS	number of segments used to approximate a closed curve
m, n	Fourier harmonic numbers associated with axial and circumferential directions, respectively
P_{mn}, P'_{mn}	load coefficients in $P_r(x, \phi)$ which is expressed in Fourier series
P, M_L, M_c	radial load, axial moment and circumferential moment, respectively
$P_r(x, \phi)$	normal (radial) load distribution function
q_0, q_1, q_2	load intensities
r	mean radius of cylinder
s	dummy parameter in the mapping function
t	thickness of cylinder
u, v, w	axial, tangential and radial displacements, respectively
λ	$m\pi r/L$
ν	Poisson's ratio
σ_x, σ_ϕ	axial and circumferential stresses, respectively
(x, ϕ)	cylindrical coordinate system
(ζ, η)	transformed coordinate system

1. INTRODUCTION

Cylindrical shell structures are subjected to a variety of local loads. These loads are often transmitted to the shells through nozzles, piping connections and welded attachments such as brackets and supports. While the cross-sections of nozzles and pipes are circular, welded attachments may be rectangular, circular, elliptical or have I, T, L or other shapes. In

†Author to whom correspondence should be addressed.

addition, the applied load on the attachment may be an axial force, a moment or both. To find the deflection and stress distributions associated with such a complex geometry and loading condition, it is necessary to express the loading and geometric details of the attachment as mathematical functions so as to facilitate a theoretical analysis of the problem.

The sets of governing equations for the cylindrical shell are often expressed in terms of load and displacement functions. In this work, the set of thin-walled cylindrical shell equations due to Sanders (1959) will be employed. Sanders' shell theory was derived via the variational principle of virtual work. It has received widespread use in recent years and is regarded by many as being the best within its class.

If only the normal radial loads on the cylinder are considered, then the cylindrical shell equations for displacements (u, v, w) can be written in the following form:

$$\begin{bmatrix} L_1 & L_2 & L_3 \\ L_2 & L_4 & L_5 \\ L_3 & L_5 & L_6 \end{bmatrix} \begin{Bmatrix} w \\ u \\ v \end{Bmatrix} = \frac{r^2}{A} \begin{Bmatrix} P_r \\ 0 \\ 0 \end{Bmatrix}, \tag{1}$$

where the L values are the differential operators of Sanders' shell theory.

A particular solution of these equations for a cylindrical shell under radial load and simply supported at the ends can be solved by the double Fourier series expansion technique [for example, in the papers of Bijlaard (1955), Duthie *et al.* (1982) and Ong (1987)]. The forms of the Fourier series are chosen so that the boundary conditions are identically satisfied. In this approach, the known loading distribution is expressed in terms of Fourier series in which the Fourier coefficients can be determined by simple formulae. The unknown displacements are also expressed in terms of double Fourier series and their coefficients can be found, in terms of loading coefficient, by solving the shell equations.

The double Fourier series for a distributed radial load (P_r) acting on the cylindrical surface can be expressed as follows:

$$P_r(x, \phi) = \sum_{m=1}^{\infty} \sum_{n=0}^{\infty} (P_{mn} \cos n\phi + P'_{mn} \sin n\phi) \sin\left(\frac{m\pi x}{L}\right). \tag{2}$$

Substituting eqn (2) into eqn (1), solutions for the displacements can be determined as follows:

$$w = \frac{r^2}{kA} \sum_{m=1}^{\infty} \sum_{n=0}^{\infty} Z1_{mn}(P_{mn} \cos n\phi + P'_{mn} \sin n\phi) \sin\left(\frac{m\pi x}{L}\right)$$

$$u = \frac{r^2}{kA} \sum_{m=1}^{\infty} \sum_{n=0}^{\infty} Z2_{mn}(P_{mn} \cos n\phi + P'_{mn} \sin n\phi) \cos\left(\frac{m\pi x}{L}\right)$$

$$v = \frac{r^2}{kA} \sum_{m=1}^{\infty} \sum_{n=0}^{\infty} Z3_{mn}(P_{mn} \sin n\phi - P'_{mn} \cos n\phi) \sin\left(\frac{m\pi x}{L}\right), \tag{3}$$

where

$$Z1_{mn} = (\lambda^2 + n^2)^2 / DEN$$

$$Z2_{mn} = -\lambda \left[n^2(\lambda^2 + n^2) \frac{2k}{1-\nu} - \lambda^2 \nu + n^2 \right] / DEN$$

$$Z3_{mn} = -n \left[\frac{3-\nu}{1-\nu} k\lambda^4 + \frac{2(2-\nu)}{1-\nu} \lambda^2 n^2 + n^4 + (2+\nu)\lambda^2 + n^2 \right] / DEN$$

$$DEN = \lambda^8 + 4n^2\lambda^6 + \left[\frac{1-v^2}{k} + 6n^2(n^2-1)\right]\lambda^4 + 4n^2(n^2-1)^2\lambda^2 + n^4(n^2-1)^2. \quad (4)$$

By the strain and curvature relationships of Sanders, the following stress and moment resultants can be obtained:

$$N_\phi = \frac{r}{k}\sum_{m=1}^{\infty}\sum_{n=0}^{\infty}[Z1_{mn} - \lambda v Z2_{mn} + nZ3_{mn}]G(m,n,x,\phi)$$

$$N_x = \frac{r}{k}\sum_{m=1}^{\infty}\sum_{n=0}^{\infty}[vZ1_{mn} - \lambda Z2_{mn} + vnZ3_{mn}]G(m,n,x,\phi)$$

$$M_\phi = r^2\sum_{m=1}^{\infty}\sum_{n=0}^{\infty}[(n^2 + v\lambda^2)Z1_{mn} + nZ3_{mn}]G(m,n,x,\phi)$$

$$M_x = r^2\sum_{m=1}^{\infty}\sum_{n=0}^{\infty}[(vn^2 + \lambda^2)Z1_{mn} + vnZ3_{mn}]G(m,n,x,\phi), \quad (5)$$

where

$$G(m,n,x,\phi) = (P_{mn}\cos n\phi + P'_{mn}\sin n\phi)\sin\left(\frac{m\pi x}{L}\right).$$

Finally, based on these stress and moment resultants, stresses on the outer and inner surfaces of the shell can be calculated as follows:

$$\sigma_x = \frac{N_x}{t} \pm \frac{6M_x}{t^2} \quad (+\text{outside}, -\text{inside})$$

$$\sigma_\phi = \frac{N_\phi}{t} \pm \frac{6M_\phi}{t^2} \quad (+\text{outside}, -\text{inside}). \quad (6)$$

The aforementioned method of solution is plausible as all solutions can be expressed in series forms and their numerical solution values can be attained by series summation. Furthermore, all solutions can be summed once the load coefficients P_{mn} and P'_{mn} are evaluated. Since the applied loads on the shell are known, its associated Fourier coefficients should be able to be determined.

The object of this paper is to search for an efficient method for evaluating the load coefficients P_{mn} and P'_{mn} for a surface radial loading applied on an arbitrarily shaped area. Two methods are proposed for the evaluation of load coefficients; their versatility, strengths and weaknesses will be discussed.

2. REPRESENTING LOADING DISTRIBUTION BY FOURIER SERIES

The general expression for the load coefficients P_{mn} and P'_{mn} can be derived directly from eqn (2), through the use of orthogonal relationships for sine and cosine functions, as follows:

$$P_{mn} = \frac{1}{L\pi}\int_0^L\int_0^{2\pi} P_r(x,\phi)\sin\left(\frac{m\pi x}{L}\right)d\phi\cdot dx \quad (m = 1,2,3,\ldots, n = 0) \quad (7a)$$

$$= \frac{2}{L\pi}\int_0^L\int_0^{2\pi} P_r(x,\phi)\cos n\phi\sin\left(\frac{m\pi x}{L}\right)d\phi\cdot dx \quad (m,n = 1,2,3,\ldots) \quad (7b)$$

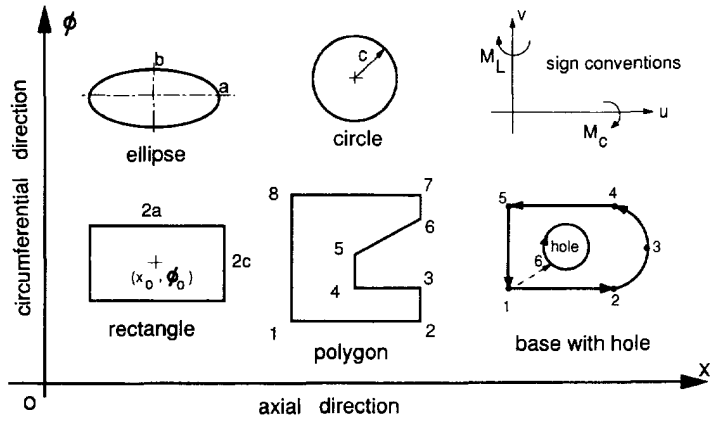

Fig. 1. Local loads with different base profiles.

$$P'_{mn} = \frac{2}{L\pi}\int_0^L \int_0^{2\pi} P_r(x,\phi)\sin n\phi \sin\left(\frac{m\pi x}{L}\right) d\phi \cdot dx \quad (m,n = 1,2,3,\ldots). \tag{7c}$$

For applied loads applied on a rectangular area, the integrals of eqns (7) are in a standard form and can be evaluated easily. As an example, the closed form expressions for P_{mn} and P'_{mn} for a load located at (x_0, ϕ_0) and of uniform intensity "q" acting over a rectangular area of axial length "$2a$" and width "$2c$", as shown in Fig. 1, are as follows:

$$P_r(x,\phi) = q \text{ in the region } \left(\phi_0 - \frac{c}{r} \leqslant \phi \leqslant \phi_0 + \frac{c}{r},\quad x_0 - a \leqslant x \leqslant x_0 + a\right) \tag{8a}$$

$$P_{mn} = \frac{4qc}{m\pi^2 r}\sin\left(\frac{m\pi x_0}{L}\right)\sin\left(\frac{m\pi a}{L}\right) \quad (m = 1,2,3,\ldots, n = 0)$$

$$= \frac{8q}{mn\pi^2}\sin\left(\frac{m\pi x_0}{L}\right)\sin\left(\frac{m\pi a}{L}\right)\cos n\phi_0 \sin\left(\frac{nc}{r}\right) \quad (m,n = 1,2,3,\ldots) \tag{8b}$$

$$P'_{mn} = \frac{8q}{mn\pi^2}\sin\left(\frac{m\pi x_0}{L}\right)\sin\left(\frac{m\pi a}{L}\right)\sin n\phi_0 \sin\left(\frac{nc}{r}\right) \quad (m,n = 1,2,3,\ldots). \tag{8c}$$

For the general case of a load acting over an arbitrarily shaped area, the integral limits of eqns (7) are variables, which means that the integrals cannot be evaluated in a direct manner. Two methods are described in the following to evaluate the double integrals in eqns (7).

2.1. *Method* I—*discrete Fourier approximation*

The load coefficients in eqn (2) can be evaluated without errors as follows:

$$P_{mn} = \frac{2}{MN}\sum_{i=1}^{M}\sum_{j=1}^{N} P_r(x_i,\phi_j)\sin\left(\frac{m\pi x_i}{L}\right) \quad (\text{for } m \geqslant 1, n = 0) \tag{9a}$$

$$= \frac{4}{MN}\sum_{i=1}^{M}\sum_{j=1}^{N} P_r(x_i,\phi_j)\cos(n\phi_j)\sin\left(\frac{m\pi x_i}{L}\right) \quad (\text{for } m,n \geqslant 1) \tag{9b}$$

$$P'_{mn} = \frac{4}{MN}\sum_{i=1}^{M}\sum_{j=1}^{N} P_r(x_i,\phi_j)\sin(n\phi_j)\sin\left(\frac{m\pi x_i}{L}\right) \quad (\text{for } m,n \geqslant 1), \tag{9c}$$

where

$$x_i = \frac{Li}{M}; \quad \phi_j = \frac{\pi j}{N}; \quad m \leqslant M/2; \quad n \leqslant N/2.$$

In the foregoing equations, the integration domain $[0 \leqslant x \leqslant L, 0 \leqslant \phi \leqslant 2\pi]$ is divided into M divisions in the x-direction and N divisions in the circumferential direction. The maximum number of Fourier harmonics that can be evaluated accurately by this technique is equal to half the number of divisions.

The discrete Fourier approximation method is in fact equivalent to applying the simple trapezoidal rule to the double integrals of eqns (7). The trapezoidal rule has been shown to be highly accurate for Fourier series. The discrete Fourier approximation technique is a general technique and can handle any force distribution. However, it is quite an inefficient and tedious method unless Fast Fourier Transform can be appropriately employed. The method requires values of $P_r(x, \phi)$ at all collocation points and double summation has to be performed for each Fourier coefficient. A great deal of computational effort is needed and thus it is not the preferred choice.

2.2. *Method* II—*contour line integral*

The double integrals of eqns (7) can be transformed into line integrals by means of Green's theorem. For the convenience of expressing the integral results, the integrands in eqns (7a–c) are defined as follows.

Let

$$f_0(x, \phi) = P_r(x, \phi) \sin\left(\frac{m\pi x}{L}\right)$$

$$f_1(x, \phi) = P_r(x, \phi) \cos n\phi \sin\left(\frac{m\pi x}{L}\right)$$

$$f_2(x, \phi) = P_r(x, \phi) \sin n\phi \sin\left(\frac{m\pi x}{L}\right). \tag{10}$$

Applying Green's theorem, $\iint_R (\partial F/\partial y)\,\mathrm{d}x \cdot \mathrm{d}y = -\oint_c F\,\mathrm{d}x$, to eqn (7) yields the following integral expressions:

$$\iint_R f_k(x, \phi)\,\mathrm{d}x \cdot \mathrm{d}\phi = \oint_C F_k(x, \phi)\,\mathrm{d}x, \tag{11a}$$

where

$$F_k(x, \phi) = -\int_0^{\phi} f_k(x, s)\,\mathrm{d}s \quad (k = 0, 1, 2) \tag{11b}$$

and C is the boundary enclosing the domain R.

The line integral is positive when it is evaluated in an anti-clockwise direction.

The load coefficients can now be evaluated by performing a line integral around the base perimeter as follows:

$$P_{mn} = \frac{1}{L\pi}\oint_C F_0(x, \phi)\,\mathrm{d}x \quad (m = 1, 2, 3 \ldots, n = 0)$$

$$= \frac{2}{L\pi}\oint_C F_1(x, \phi)\,\mathrm{d}x \quad (m, n = 1, 2, 3, \ldots)$$

$$P'_{mn} = \frac{2}{L\pi}\oint_C F_2(x, \phi)\,\mathrm{d}x \quad (m, n = 1, 2, 3, \ldots). \tag{12a–c}$$

When the external loads and moments are applied through an attachment to the shell, the force transmitted to the shell will not be uniformly distributed over the loaded area as a result of different structural rigidities between the attachment and the shell. However, in most design practices, it is customary to ignore the rigidity of the attachment in order to simplify a design procedure. Such a design simplification is equivalent to saying that the shell is able to deform freely under the applied loads. In this case, the force on the shell will be linearly distributed over the base of the attachment, as can be expressed by

$$P_r(x, \phi) = q_0 + q_1 x + q_2 \phi. \tag{13}$$

With the above load distribution, the functions $F_k(x, \phi)$, $k = 0, 1, 2$, can be evaluated as follows:

$$\begin{aligned} F_0(x, \phi) &= -\int_0^{\phi} P_r(x, s) \sin\left(\frac{m\pi x}{L}\right) \mathrm{d}s \\ &= -\int_0^{\phi} (q_0 + q_1 x + c_2 s) \sin\left(\frac{m\pi x}{L}\right) \mathrm{d}s \\ &= -[(q_0 + q_1 x)\phi + \tfrac{1}{2} q_2 \phi^2] \sin\left(\frac{m\pi x}{L}\right) \end{aligned} \tag{14a}$$

$$\begin{aligned} F_1(x, \phi) &= -\int_0^{\phi} P_r(x, s) \cos(ns) \sin\left(\frac{m\pi x}{L}\right) \mathrm{d}s \\ &= -\frac{1}{n^2} [(q_0 + q_1 x) n \sin n\phi + q_2 (\cos n\phi + n\phi \sin n\phi - 1)] \sin\left(\frac{m\pi x}{L}\right) \end{aligned} \tag{14b}$$

$$\begin{aligned} F_2(x, \phi) &= -\int_0^{\phi} P_r(x, s) \sin(ns) \sin\left(\frac{m\pi x}{L}\right) \mathrm{d}s \\ &= -\frac{1}{n^2} [(q_0 + q_1 x) n (1 - \cos n\phi) + q_2 (\sin n\phi - n\phi \cos n\phi)] \sin\left(\frac{m\pi x}{L}\right). \end{aligned} \tag{14c}$$

We are now in a position to evaluate the load coefficients P_{mn} and P'_{mn} using eqns (12a–c).

For a circular or elliptical base profile, the base profile can be expressed mathematically. In this case, eqns (12) can be evaluated directly without discretization of the boundary curve. The boundary coordinates for an elliptical load located at (x_0, ϕ_0), with a major axis "$2a$" and minor axis "$2b$", can be expressed as follows:

$$x = a \cos\theta + x_0, \quad \phi = \left(\frac{b}{r}\right) \sin\theta + \phi_0; \quad [0, 2\pi] \in \theta. \tag{15a}$$

The line integral over the range $[0, 2\pi]$ can be mapped into the range $[-1, 1]$ by the following transformations:

$$\theta = \pi(1 + s), \quad \mathrm{d}x = -(a\pi \sin\theta)\, \mathrm{d}s; \quad [-1, 1] \in s. \tag{15b}$$

The circular shaped base with a radius "c" is a special case of the elliptical base by setting $c = a = b$. It is either impossible or not easy to evaluate eqns (12) directly if the base profile is a general shape made up of a series of straight and curve line segments, such as some of

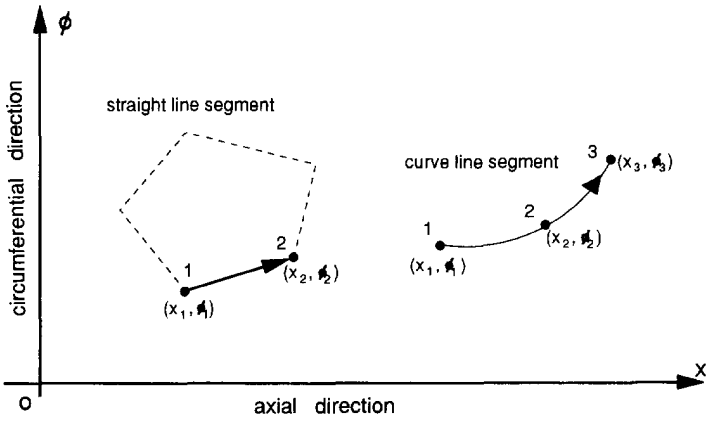

Fig. 2. Base profiles approximated by line segments.

the shapes shown in Fig. 2. In this case, the contour integral must be carried out along each line segment in order to obtain the total integral result. The load coefficients can be rewritten as follows:

$$P_{mn} = \frac{1}{L\pi}\sum_{1}^{NS}\int_{-1}^{1} F_0(x,\phi)\,\mathrm{d}s \quad (m = 1,2,3,\ldots,n = 0)$$

$$= \frac{2}{L\pi}\sum_{1}^{NS}\int_{-1}^{1} F_1(x,\phi)\,\mathrm{d}s \quad (m,n = 1,2,3,\ldots)$$

$$P'_{mn} = \frac{2}{L\pi}\sum_{1}^{NS}\int_{-1}^{1} F_2(x,\phi)\,\mathrm{d}s \quad (m,n = 1,2,3,\ldots), \tag{16a–c}$$

where NS is the number of segments around the base profile.

The line segment joining points (x_1, ϕ_1) and (x_2, ϕ_2), as shown in Fig. 2, can be mapped into the interval $s \in [-1, 1]$ through the following transformations:

$$x = \tfrac{1}{2}[(x_1 + x_2) + (x_2 - x_1)s]$$
$$\phi = \tfrac{1}{2}[(\phi_1 + \phi_2) + (\phi_2 - \phi_1)s]$$
$$\mathrm{d}x = \tfrac{1}{2}(x_2 - x_1)\,\mathrm{d}s. \tag{17}$$

Similarly, a curve segment joining three points (x_1, ϕ_1), (x_2, ϕ_2) and (x_3, ϕ_3), as shown in Fig. 2, can be mapped into the interval $s \in [-1, 1]$ through the following transformations:

$$x = \tfrac{1}{2}[2x_2 + (x_3 - x_1)s + (x_1 - 2x_2 + x_3)s^2]$$
$$\phi = \tfrac{1}{2}[2\phi_2 + (\phi_3 - \phi_1)s + (\phi_1 - 2\phi_2 + \phi_3)s^2]$$
$$\mathrm{d}x = [\tfrac{1}{2}(x_3 - x_1) + (x_3 - 2x_2 + x_1)s]\,\mathrm{d}s. \tag{18}$$

Integral expressions of eqns (12) and (16) can be evaluated by the Clenshaw–Curtis (1993) quadrature rule. This method approximates the integrand by Chebyshev polynomials on the interval $[-1, 1]$. Each polynomial is then integrated exactly. The method is numerically stable to a high degree and is comparable in accuracy to that by an equivalent Gaussian rule. It can be shown that it is exact for polynomials of degree N or less. The most attractive feature of this method is that it is completely self-contained, requiring no tabulated values for quadrature weights and points. Any degree of approximation can be obtained and

checked for its accuracy. The method has been found to be successful for a wide range of integrals because the Chebyshev series approximation is very good in the interval $[-1, 1]$.

The Clenshaw–Curtis quadrature rule can be expressed as follows:

$$I = \int_{-1}^{1} f(s)\,\mathrm{d}s$$

$$I_N = -\frac{4}{N}\sum_{k=0}^{N}{}''f\left(\cos\frac{\pi k}{N}\right)\sum_{j=0}^{N}{}''\frac{1}{j^2-1}\cdot\cos\frac{\pi jk}{N} \quad (j = 0, 2, 4, \ldots; \text{even terms only}), \tag{19}$$

where I_N is the N-term approximation of the integral; the double prime $''$ indicates that the first and last terms of the series are to be halved.

It has to be mentioned here that although the sine and cosine functions exhibit highly oscillatory behaviour, which leaves only the very high order quadrature methods with any chance of success, no such difficulty is encountered in the present work. The degree of oscillation may be high with respect to the entire region of the shell surface, but it is definitely low over the loaded area. For this reason, there is no numerical instability associated with integration of the sine and cosine functions. It has been found that the 10–20-term approximation used in eqn (19) would give sufficient accuracy for most loading cases.

If the function $f(x)$ in eqn (11b) cannot be integrated analytically in the case of a complex load distribution function $P_r(x, \phi)$, a numerical integration method can be employed to evaluate the double integrals of eqn (7). For a base profile consisting of a series of straight line segments, as shown in Fig. 3, the result of the integral is the sum of projected areas under all line segments, which takes into account the sign of the integration. The projected area under each line segment is a trapezoidal shape which can be transformed into the square domain $[\zeta, \eta]$, as shown in Fig. 3. The transformation is necessary if a standard numerical quadrature integration rule is to be used. The load coefficients are then expressed as follows:

$$P_{mn} = \frac{1}{L\pi}\sum_{1}^{NS}\int_{-1}^{1}\int_{-1}^{1} f_0(x,\phi)\cdot\det(J)\cdot\mathrm{d}\zeta\cdot\mathrm{d}\eta \quad (m = 1, 2, 3, \ldots, n = 0) \tag{20a}$$

$$= \frac{2}{L\pi}\sum_{1}^{NS}\int_{-1}^{1}\int_{-1}^{1} f_1(x,\phi)\cdot\det(J)\cdot\mathrm{d}\zeta\cdot\mathrm{d}\eta \quad (m, n = 1, 2, 3, \ldots) \tag{20b}$$

$$P'_{mn} = \frac{2}{L\pi}\sum_{1}^{NS}\int_{-1}^{1}\int_{-1}^{1} f_2(x,\phi)\cdot\det(J)\cdot\mathrm{d}\zeta\cdot\mathrm{d}\eta \quad (m, n = 1, 2, 3, \ldots), \tag{20c}$$

where $\det(J)$ is the Jacobian determinant for the transformation from (x, ϕ) to (ζ, η).

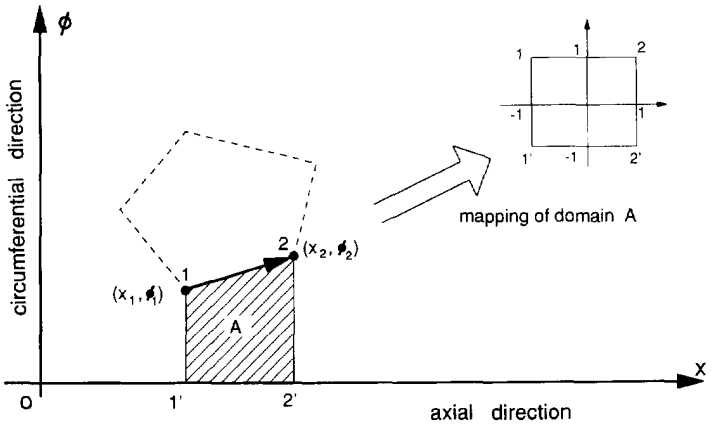

Fig. 3. Mapping of a domain for integration.

Functions $f_k(x, \phi)$ in eqns (20) can be mapped into $f(\zeta, \eta)$ through the following transformations:

$$x = \tfrac{1}{2}[(x_1 + x_2) + (x_2 - x_1)\zeta]$$
$$\phi = \tfrac{1}{4}(1+\eta)[(\phi_1 + \phi_2) + (\phi_2 - \phi_1)\zeta]$$
$$\det(J) = \tfrac{1}{8}(x_2 - x_1)[(\phi_1 + \phi_2) + (\phi_2 - \phi_1)\zeta]. \tag{21}$$

3. RELATIONSHIP BETWEEN APPLIED LOADS AND LOAD DISTRIBUTION FUNCTION

In order to derive a simple relationship between loads applied on the attachment and its resulting force distribution on the shell surface, it is assumed here that the shell is free to deform under load. In other words, the structural rigidity of the attachment will not be considered. In reality, the force distribution on the shell due to external loads acting on a rigid attachment will never be uniformly distributed over the base of the attachment. A high concentration of forces will occur around the edges of the attachment. Nevertheless, local thickening or reinforcement of the shell at the structural junctions will also alleviate the stress concentration due to the structural discontinuity.

If the structural rigidity of the attachment is neglected, then the force on the cylindrical shell will follow the nominal bending stress pattern of the attachment at its base. This simplifying assumption has been adopted by most pressure vessel design codes as a basis for dealing with the local loading problems. For example, the reaction force distribution on the shell surface due to an applied moment on a rectangular attachment is always assumed to vary linearly across the base of the attachment. This implies that the attachment is very flexible and it does not impose restraint on the shell displacements. In recognizing the fact that local stress concentrations do exist at the structural junctions, desgin codes usually specify allowable stress limits on the stresses calculated based on the flexible attachment's assumption.

For an attachment of arbitrary shaped base, the sectional properties such as the centroid and the moments of areas can be determined. The nominal force distribution at the base of the attachment can then be found by the engineer's beam theory. In the following, the force distributions at the base of two attachments, one with a rectangular base and the other with an elliptical base, will be derived when they are subjected to combined external loads consisting of a direct load P, an axial moment M_L and a circumferential moment M_c.

(a) Rectangular base profile with centroid located at (x_0, ϕ_0):

$$I_u = \tfrac{4}{3}ac^3, \quad I_v = \tfrac{4}{3}a^3c,$$
$$P_r(x, \phi) = \frac{P}{4ac} + \left(\frac{3M_L}{4a^3c}\right)(x - x_0) + \left(\frac{3M_c r}{4ac^3}\right)(\phi - \phi_0). \tag{22}$$

(b) Elliptical base profile with centroid located at (x_0, ϕ_0):

$$I_u = \frac{\pi}{4}ab^3, \quad I_v = \frac{\pi}{4}a^3b,$$
$$P_r(x, \phi) = \frac{P}{\pi ab} + \left(\frac{4M_L}{\pi a^3 b}\right)(x - x_0) + \left(\frac{4M_c r}{\pi ab^3}\right)(\phi - \phi_0). \tag{23}$$

Load distribution for attachments with other base profiles can be determined in a similar manner. For a base area having no axis of symmetry, as in a case of an "L"-shaped

attachment, it is necessary to use the general beam bending theory applicable to an unsymmetrical section to find the load distribution function.

4. VERIFICATION OF THE PRESENT APPROACH

The discrete Fourier approximation method has been adopted by Tooth *et al.* (1989) to evaluate Fourier coefficients associated with thermal loadings on a cylindrical shell. They compared their theoretical results with the finite element method and very good agreement was obtained between the two. The discrete Fourier approximation method is thus a very reliable and accurate method for evaluating Fourier load coefficients. However, as mentioned before, this method requires a great deal of computational effort and data management and is thus not the preferred choice. The following section will therefore focus on the verification of Method II—the contour line integral method.

In order to validate the contour line integral method for evaluating Fourier load coefficients, a comparison of computed results with those of Nash *et al.* (1991) for a circular base profile is presented here. Nash *et al.* (1991) evaluated the load coefficients for the circular patch by direct integration involving variable integral limits. Such an approach is feasible only when the shape is well defined, such as a circle or an ellipse. The method becomes difficult or impossible for a general shape.

The cylindrical shell has a mean radius $r = 28$ in, thickness $t = 1.3$ in and length $L = 71$ in; the circular attachment has a mean radius $c = 5.4375$ in. The Young's modulus $E = 30 \times 10^6$ lb in.$^{-2}$ and Poisson's ratio $v = 0.3$. The shell is subjected to three separate load cases: a radial load of 94,900 lb, a circumferential moment of 410,000 in-lb and an axial moment of 410,000 in-lb.

A comparison between the present approach and that of Nash *et al.* (1991) is given in Table 1. In the case of the circular patch load, the results are computed at the centre of the patch; for the applied moments, the results are computed at the edge of the patch. It can be seen that very good agreement is found.

Also shown in Table 1 are the results for an equivalent square base. The concept of an equivalent base has been adopted by most pressure vessel design codes to convert circular and elliptical base profiles to a standard rectangular or square shape for which tabulated results are available. Herein, the half-width of the equivalent square is taken as $0.876r$, obtained from Timoshenko and Woinowsky-Krieger (1981) on the basis of an equal centroidal stress value between circular and square patch loads applied on a simply supported plate. Table 1 shows that the equivalent square concept gives good agreement for the radial load case; however, for applied moments, more than 10% error on stresses is incurred.

Table 1. Comparison of results for loads on a circular base ($r = 28$ in, $t = 1.3$ in, $L = 71$ in, $c = 5.4375$ in)

Radial patch ($P = 94{,}900$ lb)	$N_x(r/P)$	$N_\phi(r/P)$	M_x/P	M_ϕ/P	σ_x (psi)	σ_ϕ (psi)
Nash *et al.* (1991)	−2.924	−3.353	0.064	0.088	−29329	−38474
Equivalent square	−2.921	−2.947	0.062	0.087	−28659	−37241
Present	−2.915	−2.963	0.062	0.087	−28533	−37213
Cir. moment ($M_c = 410{,}000$ in-lb)	$N_x(cr/M_c)$	$N_\phi(cr/M_c)$	$M_x(c/M_c)$	$M_\phi(c/M_c)$	σ_x	σ_ϕ
Nash *et al.* (1991)	−1.560	−0.998	0.067	0.102	−21065	−29294
Equivalent square	−1.393	−0.764	0.057	0.104	−18266	−29573
Present	−1.542	−0.989	0.067	0.102	−20821	−28900
Axial moment ($M_L = 410{,}000$ in-lb)	$N_x(cr/M_L)$	$N_\phi(cr/M_L)$	$M_x(c/M_L)$	$M_\phi(c/M_L)$	σ_x	σ_ϕ
Nash *et al.* (1991)	−0.965	2.871	0.068	0.056	−20147	−20977
Equivalent square	−0.866	2.695	0.070	0.046	−20443	−17986
Present	−0.963	2.584	0.065	0.055	−19341	−20148

Table 2. Convergence of numerical integration for a circular patch load ($r = 28$ in, $t = 1.3$ in, $L = 71$ in, $c = 5.4375$ in)

Quadrature points	$N_x(r/P)$	$N_\phi(r/P)$	M_x/P	M_ϕ/P
10	−2.915	−2.907	0.054	0.085
20	−2.915	−2.963	0.061	0.087
50	−2.915	−2.963	0.062	0.087
100	−2.915	−2.963	0.062	0.087

The contour line integral method is also validated against eqn (8) for a rectangular patch under uniform pressure q_0. In this case, perfect agreement is attained. However, the contour line method requires greater computation time compared to direct use of eqn (8) because for each Fourier coefficient, four line integrations have to be performed.

Perhaps the greatest advantage of the contour line integral method is that it can handle complex shape and complex loading distribution systems readily with ease and without further computational effort. For example, an attachment with an irregularly shaped base is subject to load and moments simultaneously. For such a case, the discrete Fourier method would require reformulation or modification of the programming codes.

One of the main concerns of the contour integral method is the reliability of the numerical integration rule; for the present case, the Clenshaw–Curtis quadrature rule. To show the convergence of integral results, the circular patch is used here as a case example. As the circle has an analytical expression, there is no requirement to partition the circular boundary into several segments for the purpose of integration. The integration limits $[0, 2\pi]$ are transformed into $[-1, 1]$ using eqn (15). Table 2 shows the convergence of the integral results. It is seen that for the present example, 25 integration points around the circle are enough for an accurate result.

The same circular patch is used again to validate the curve line segment. The boundary of the circle is modelled by two, four and eight curve segments, respectively. The results are given in Table 3. It can be inferred from the results that at least four curve line segments must be used to model a complete circular boundary. When only two curve segments are used, nearly 10% errors in the results are incurred. This verification example thus validates the use and limitation of the curve line segment.

Provision of straight and curve segments permits modelling of a complex base profile with ease. As mapping is performed on each line segment individually, the contour line integral method can handle profiles with concave and convex corners. In fact, any advantage derived from the line integral principle will be applicable here. For example, in the case of a base with internal holes, artificial lines can be constructed to connect external and internal regions and the line integral can be carried out over contours of all regions.

5. CONCLUSIONS

The problem of a cylindrical shell subject to local loads with an arbitrary base profile has been studied in this article. Solutions for stresses and displacements are derived and expressed by double Fourier series. Two general methods are studied to evaluate the Fourier load coefficients for loads with an arbitrary shaped base. The first is the discrete Fourier approximation method, which requires much computational effort and data management

Table 3. Validation of curve line segment for a circular base ($r = 28$ in, $t = 1.3$ in, $L = 71$ in, $c = 5.4375$ in)

No. of curve segments (NS)	$N_x(r/P)$	$N_\phi(r/P)$	M_x/P	M_ϕ/P	σ_x (psi)	σ_ϕ (psi)
2	−2.524	−3.353	0.058	0.079	−26317	−33686
4	−2.886	−2.938	0.062	0.087	−28367	−36972
8	−2.913	−2.962	0.062	0.087	−28522	−37197

on the computer; it is not a preferred choice. The second is the boundary line integral method, which is simpler to implement on the computer and which can handle complex boundary profile and loading distribution with ease. A few numerical examples show that the boundary integral method is accurate and versatile.

REFERENCES

Bijlaard, P. P. (1955). Stresses from local loadings in cylindrical pressure vessels. *Trans. ASME* **77**, 805–816.

Duthie, G., White, G. C. and Tooth, A. S. (1982). An analysis for cylindrical vessels under local loading—application to the saddle supported vessel problems. *J. Strain Anal.* **17**, 157–168.

Evans, G. (1993). *Practical Numerical Integration.* John Wiley, New York.

Nash, D. A., Tooth, A. S. and Dauda, T. (1991). The local loading of circular and elliptical attachments on cylindrical pressure vessels. *PVP*, Vol. 217, *Pressure Vessels and Components*. ASME, Philadelphia.

Ong, L. S. (1987). A computer program for cylindrical shell analysis. *Int. J. Press. Vess. Piping* **30**, 131–149.

Sanders, J. R. (1959). An improved first-approximation theory for thin shells. NASA Report No. 24.

Timoshenko, S. P. and Woinowsky-Krieger, S. (1981). *Theory of Plates and Shells*, 2nd edn, pp. 105–111. McGraw-Hill, New York.

Tooth, A. S., Panayotti, A. and Owen, R. (1989). The thermal behaviour of thin cylindrical shells—I. Heat transfer and harmonic analysis. *Int. J. Mech. Sci.* **31**, 693–706.